Anomalous small-angle x-ray scattering determination of the partial structure factors and kinetic study of unmixed Cu-Ni-Fe alloys

O. Lyon
Laboratoire de Métallurgie Physique et Laboratoire pour l'Utilisation du Rayonnement Electromagnétique, 91405 Orsay, France

J. P. Simon
Laboratoire de Thermodynamique et Physico-Chimie Métallurgiques Institut National Polytechnique de Grenoble, B.P. 75, 38402 Saint Martin-D'heres, France

(Received 28 July 1986)

Different unmixed states of a Cu-Ni-Fe alloy have been studied by anomalous small-angle x-ray scattering (ASAXS). The data were obtained at different x-ray energies near the Fe and Ni absorption edges: ASAXS intensities increase by a factor of 3, varying with the atomic contrast (with respect to Cu). Various methods for the determination of partial structure factors (PSF) have been tested and results are found reliable if we use the intensity data in the proximity of at least two edges. The homoatomic PSF curves have similar shapes with a maximum I_m which increases and shifts towards lower q values as the power laws $I_m \sim t^{0.80}$ and $q_m \sim t^{-0.26}$, and the scaling behavior is obeyed. These features are very similar to the ones observed during late stages of aging of concentrated binary systems. On the other hand, there is evidence that the phase separation of Cu-Ni-$Fe_{0.15}$ at 500 °C cannot be modeled by a two-phase system, and different possible partitioning of Cu, Ni, and Fe are discussed.

I. INTRODUCTION

The theory of the kinetics of phase separation, including problems of metastability and instability, has received considerable attention in recent years (for a review see Refs. 1 and 2). Although the various approaches are rather different, compare for example the coarse grain method, cluster dynamics, or Monte Carlo simulations of the three-dimensional Ising model, there is uncertainty when deciding which one should be applied in a specific case. In binary metallic alloys, the object size is rather small (10—100 Å) and few techniques are then available. Small-angle scattering (SAS) is one of them but this does not give a sensitive test of these theories.

Moreover, several ternary alloys have been studied as if they were pseudobinary, in particular the Cu-Ni-Fe alloys (rich in Cu and Ni): a regular pattern of phases aligned along the ⟨100⟩ directions was observed by transmission electron microscopy[3] and from this "tweedlike" morphology the existence of spinodal decomposition was claimed. Nevertheless, recent calculations have shown that elastic interactions can promote this regular morphology, independently of the unmixing mechanism.[4] The kinetics of the growth of side bands[5] and the kinetics of small-angle neutron scattering (SANS) patterns[6] follow power-law growth rather than exponential growth. Atom probe analysis combined with field emission imaging[7] yielded evidence for a separation in rather well-defined domains even at the early stages of unmixing, in disagreement with the classical spinodal decomposition model. The "phases" were, respectively, enriched in Cu and NiFe in agreement with the computed metastable fcc phase diagram.[8] As we will see, anomalous small-angle x-ray scattering (ASAXS) can be used to check the validity of the pseudobinary unmixing hypothesis in ternary alloys and may provide new information on the different solute partitioning, thanks to the determination of partial structure factors (PSF). Indeed the scattered intensity from a ternary alloy is a linear combination of these PSF, which are the Fourier transforms of the three linearly independent pair correlation functions. The extraction of the PSF needs a set of independent intensity data and this can be, in principle, achieved straightforwardly by using synchrotron radiation: The atomic scattering factor of one of the sample elements can be modified by tuning the x-ray energy to the immediate vicinity of the corresponding absorption edge. This technique is becoming widely applied in different fields of materials science.[9]

ASAXS tests were performed on binary Al-Zn alloys,[10] which have shown this technique to be quantitative. PSF determinations have been attempted on an unmixed Al-Zn-Ag alloy.[11(a)] But, since only the Zn absorption edge could be used, this led to weighted sums of the PSF.[11(b)] Nonetheless, from such measurements done on a single edge, interesting information can be obtained on the tie lines and their variations with the precipitate nature.[12]

We have chosen to study Cu-Ni-Fe alloys because this unmixing system, which has already been studied by different techniques[4–8] has two absorption edges easily available: the Fe one at 7112 eV and the Ni one at 8333 eV. This paper details and completes the results which have been shortly presented in Ref. 13. After a recall of the theoretical background and of the experimental conditions, the results appear as follows. The PSF determina-

tion, its reliability and the consequences on the unmixing morphology are treated; then the kinetic aspects are discussed.

II. THEORETICAL BACKGROUND

We have chosen to extend this presentation since this presentation is somewhat different from the one used in our previous papers.[11-14]

In the kinematical approximation, the scattered amplitude for a $(n+1)$ multicomponent system is

$$A(\mathbf{q})=\int_V \sum_{i=0}^{n} f_i \tilde{C}_i(\mathbf{R}) e^{i\mathbf{q}\cdot\mathbf{R}} d^3\mathbf{R}$$
$$=\sum_{i=0}^{n} f_i C_i(\mathbf{q}) \quad \text{with } C_i(\mathbf{q})=\mathcal{F}\{\tilde{C}_i(\mathbf{R})\} , \tag{1}$$

$\mathbf{q}$ being a reciprocal vector. In this formula f_i is the atomic scattering factor of specie i (independent from $|q|$ in the small-angle range). We have also assumed a continuum medium without a loss of generality and we will note $A^*(\mathbf{q})$ the complex conjugate of $A(\mathbf{q})$.

In the case of short-range order, the scattered intensity is taken as the thermodynamical average $\langle A(\mathbf{q})A^*(\mathbf{q})\rangle$,[13] since fluctuations in time of atomic positions can be important. However, for clustering systems measured in a frozen state, this is no longer true. Then

$$I(\mathbf{q})=\sum_{i=0}^{n} f_i C_i(\mathbf{q}) \sum_{j=0}^{n} f_j^* C_j^*(\mathbf{q}) \tag{2}$$

since $\mathcal{F}\{\sum_i \tilde{C}_i(\mathbf{R})\}=\delta(\mathbf{q})$ we can rewrite (2), with the notation

$$\tilde{F}_i=f_i-f_0=F_i e^{i\varphi_i} \text{ and } C_i(\mathbf{q})=C_i(\mathbf{q})e^{i\theta_i(\mathbf{q})} ,$$
$$I(\mathbf{q})=\sum_{i,j=1}^{n} F_i F_j e^{i(\varphi_i-\varphi_j)} C_i(\mathbf{q})C_j(\mathbf{q}) e^{i[\theta_i(\mathbf{q})-\theta_j(\mathbf{q})]} . \tag{3}$$

For a ternary alloy, this leads to

$$I(\mathbf{q})=F_1^2 C_1^2(\mathbf{q})$$
$$+2F_1F_2C_1(\mathbf{q})C_2(\mathbf{q})\cos[\varphi+\theta(\mathbf{q})]+F_2^2C_2^2(\mathbf{q}) , \tag{4}$$

where $\varphi=\varphi_2-\varphi_1$ and $\theta(\mathbf{q})=\theta_2(\mathbf{q})-\theta_1(\mathbf{q})$. This implies that, until the concentration profiles are not centrosymmetric [then $\tilde{C}_i(\mathbf{R})=\tilde{C}_i(-\mathbf{R})$ and $C_i(\mathbf{q})=C_i^*(-\mathbf{q})$], we may have a dependence of the scattered intensity with the sign of $\mathbf{q}$. Such effects are used by crystallographs in the phase-determination problem.

Since we are dealing with unoriented polycrystal samples, the same probability exists to find $\mathbf{q}$ and $-\mathbf{q}$ orientations which by adding and averaging yields to

$$I(q)=F_1^2\langle C_1^2(\mathbf{q})\rangle+2F_1F_2\cos\varphi\langle C_1(\mathbf{q})C_2(\mathbf{q})\cos\theta(\mathbf{q})\rangle$$
$$+F_2^2\langle C_2^2(\mathbf{q})\rangle . \tag{5}$$

The brackets stand for an average on all orientations of the crystals in the sample and q now stands for the modulus of the scattering vector. Rewritten in terms of PSF, we will find the condition

$$I(q)=F_1^2S_{11}(q)+2F_1F_2\cos\varphi S_{12}(q)+F_2^2(q)S_{22}(q) \tag{6}$$

with

$$S_{ii}(q)>0 \text{ and } S_{ij}^2-S_{ii}S_{jj}\le 0 . \tag{7}$$

Let us remark that this relation is actually fundamental since it is obviously independent of the particular i or j chosen, which means that

$$S_{01}^2-S_{00}S_{11}=S_{02}^2-S_{00}S_{22}$$
$$=S_{12}^2-S_{11}S_{22}\le 0 .$$

The equality $S_{ij}^2-S_{ii}S_{jj}=0$ is obtained only in special cases: isotropic monocrystals or pseudobinary systems for which all $C_i(q)$ are proportional, or finally when we consider that well-defined precipitates result from the unmixing process.

In this last case, further generalization of the equation derived in our previous paper,[14] leads to the following PSF of a $(m+1)$ phase system (m different kinds of precipitates plus a matrix):

$$S_{ij}(q)=\sum_{k,l=1}^{m} \Delta C_k^i \Delta C_l^j \psi_{kl}(q) . \tag{8}$$

ΔC_k^i is the concentration difference in element i between the phase k and the matrix 0, and $\psi_{kl}(q)$ is the Fourier transform of the pair correlation function between phases k and l.

If the decomposition of the ternary alloy gives one type of precipitates ($m=1$), all S_{ij} are proportional to the structure function of the precipitates, S_{pm}, and, through equation (8), it shortens to

$$S_{ij}(q)=\Delta C_i \Delta C_j S_{pm}(q) .$$

The case of two different kinds of precipitates should also be considered. Let us rewrite Eq. (8) with the notations

$$\lambda(q)=(\Delta C_1^1)^2\psi_{11}(q) ;$$
$$\mu(q)=\Delta C_1^1\Delta C_1^2\psi_{12}(q) ;$$
$$\nu(q)=(\Delta C_2^2)^2\psi_{22}(q) ,$$

with $\alpha_{i=1,2}=(\Delta C_i^2/\Delta C_i^1)$, α_i being the equivalent of the tie-line slope of the i phase with respect to the matrix. Then it comes to

$$S_{11}(q)=\lambda(q)+2\mu(q)+\nu(q) ,$$
$$S_{12}(q)=\alpha_1\lambda(q)+(\alpha_1+\alpha_2)\mu(q)+\alpha_2\nu(q) , \tag{9}$$
$$S_{22}(q)=\alpha_1^2\lambda(q)+2\alpha_1\alpha_2\mu(q)+\alpha_2^2\nu(q) .$$

This system of equations becomes singular if $\alpha_1=\alpha_2$, meaning that with two different kinds of precipitates located on the same pseudo-tie-line, the system can be assimilated to one with two phases. Then the relation $S_{12}^2-S_{11}S_{22}=0$ again holds.

A. Extraction of the partial structure functions

The basic idea for solving Eq. (6) in terms of PSF is to perform at least three different experiments corresponding to three different values of the atomic scattering factors,

using the anomalous effect: indeed when the x-ray energy is tuned to the immediate vicinity of one of the element absorption edges, the corresponding atomic scattering factor changes and becomes complex:

$$f=Z+f'+if'' .$$

The real part of the anomalous correction, f', can be as large as -8 electrons near a K absorption edge.

Even so, the matrix of the system of linear equations (6) is far from being well conditioned and we can expect large error amplifications when inverting the system. Several methods have been proposed to overcome this difficulty. The easiest one consists in choosing three different x-ray energies so as to optimize the conditioning of the matrix (measured for example by its Turing number). The drawback of this method is that the solution consistency cannot be checked, only through the appearance of unphysical results.[14] The other methods use an overdimensioned system by recording more than three scattering spectra. The new system of equations is then

$$\mathcal{N}(q)=\sum_{E_x=1}^{n}\left[I(q,E_x)-\sum_{i,j=1}^{2}F_i(E_x)F_j(E_x)\times\cos(\varphi_{ij})S_{ij}(q)\right]^2 . \quad (10)$$

However, since the added spectra are less and less independent, the resulting matrix is even more ill conditioned.[14] One possibility is to reduce the dimension of the system which can be done by two different ways. The first one proposed by Schevchick[16] is to determine the derivatives of intensities versus the photon energy which yields a better conditioned matrix, from which weighted sums of the PSF are extracted. It has been demonstrated that, for a given amplitude of error, this method is much more precise than the direct one. Unfortunately, what is gained by it, is obviously lost when calculating the derivatives.

An alternative to this method[14] can be applied when the relative variations of atomic scattering factors are small enough, such as the quadratic term $(\Delta F_i/\bar{F}_i)^2$ in Eq. (10) can be either neglected, or replaced by its average value [idem for the $\cos\varphi(E)$ term]. Then from the slope and the intercept of the variation of $I(q,E)$ versus $\Delta F_i(E)/\bar{F}_i$, new sets of weighted sums of the PSF are determined. In the case of the Cu-Ni-Fe alloys, our method cannot be applied since the $\bar{F}_i$, of the same order of magnitude as Z_i-Z_{Cu}, are rather small. This leads to rather large values of $\Delta F_i/\bar{F}_i$ and dropping the $(\Delta\bar{F}_i/F_i)^2$ term is no longer a wise idea.

This is why we chose the direct method but with a more refined method: first we determined the PSF by inverting the system of Eq. (10), then the resulting $S_{ij}(q)$ were used as a starting point to determine the true minimum of $\mathcal{N}(q)$ by a gradient method.

The last question is how many different energies should be used for each absorption edge. Following Refs. 17 and 18, it seems that adding more than five does not improve the results although one tends to think that an extra one would reduce the statistic uncertainty. In practice, we chose seven different energies on each edge so as to be able to disregard eventual erroneous measurements. This was done by inspection of the plots $\sum_q I(q,E)$ versus $F_1(E)$ or $F_2(E)$ and by removing experiments far from the general trend. Another advantage is to test the sensitivity of the results, due to the choice of the retained anomalous measurements.

III. EXPERIMENTAL CONSIDERATIONS

A. Sample preparation

The alloy was prepared from 99.99% pure disoxydized metals by semi-levitation under pure argon and chill cast in a copper ingot. The homogeneity was controlled by x-ray analysis in SEM and the final composition, checked on the samples themselves, was $Cu_{0.426}Ni_{0.422}Fe_{0.152}$. After rolling down to about 50 μm, the material was homogenized during 0.5 h at 850 °C in evacuated capsules and water quenched. After final electrochemical thinning, the samples now 20 μm thick were isothermally aged at 500 °C under secondary vacuum during 3, 9, and 56 h, respectively.

B. Apparatus

ASAXS experiments were performed at Laboratoire pour l'Utilisation du Rayonnement Electromagnétique (LURE) on beam line D22.[19] The double monochromator was calibrated by determining the inflection point of the absorption edges of Fe and Ni, which values are tabulated at 7112 and 8333 eV. The stability of the experimental setup was better than 1 eV when going from one edge to the other. The experimental setup was nearly the same as described in our previous study,[11] but since we expected much lower scattered intensities, a few changes were made to minimize parasitic scattering: we kept the upstream scintillator monitoring the primary beam intensity M but we removed the backward ionization chamber in order that the whole beam would be under vacuum after the sample. The drawback was that the sample transmissions versus energy had to be measured after collecting the spectra. This was done by replacing the position sensitive detector by the ionization chamber, but without changing the sample position so as to avoid any error coming from possible heterogeneities of its thickness.

C. Data correction

From these transmission measurements $T(E)$ done at different energies E and from corresponding data of the absorption coefficients, we were able to determine the sample thickness t within 1% square deviation in every case. The classical correction formula is given to emphasize the importance of the different parameters:

$$I(q,E)=E_f(q)E_f(E)\,|\,I_s/M_sT(E)-I_p/M_p\ \ (1/t) .$$

I_s is the scattering intensity of the sample, M_s the corresponding monitoring, and I_p is the residual scattering without sample for a monitoring M_p. $E_f(q)$ is the detector efficiency versus position: it was determined with the

flat fluorescence spectrum of a Cu thin foil recorded above its absorption edge. $E_f(E)$, the detector efficiency versus energy was controlled through nonanomalous spectra of an Al-Zn-Ag alloy. An important correction to the data (which might have been troublesome but in fact was not) was the Fe fluorescence which appears when studying the Ni absorption edge. Since the used x-ray energy is only about 1 keV above the Fe absorption edge, the Fe fluorescence cannot be discriminated by the detector energy analyzer which resolution is around 20%. Nevertheless, the fluorescence gave a flat background which was easily removed from the spectra since the sample signal was negligible above $q = 0.35$ Å^{-1} (see Fig. 1 uncorrected for fluorescence).

D. Atomic scattering factors

Last but not least, we needed to know the values of $f'(E)$ and $f''(E)$. For these we used data[20] computed from absorption coefficients through the optical theorem and the Kramer-Kronig integral. So as to avoid any discrepancy between real and tabulated values, we set the closest energy to about 10 eV below each edge. Furthermore, f' values were checked by running ASAXS experiments on binary unmixed alloys ($Fe_{0.65}Cr_{0.35}$ for the Fe edge and $Ni_{0.86}Al_{0.14}$ for the Ni one). Both data fit together within 0.2 electron (see Table I).

IV. EXPERIMENTAL RESULTS

Having made all the corrections, the ASAXS spectra vary with energy as shown in Figs. 1(a) and 1(b) (for example, in the case of Cu-Ni-$Fe_{0.15}$ aged 56 h at 500 °C). Near both Fe and Ni absorption edges, the scattered intensity for a given q vector increases rapidly when coming up to the edge. This is qualitatively consistent with the corresponding increase of the difference between the Cu and the Fe or the Cu and the Ni atomic scattering factors. At first glance, all $I(q,E)$ curves appear the same, as if they

TABLE I. Atomic sattering contrasts (with respect to Cu atomic scattering factor).

E (eV)	$\|\|F_1\|\|$	$\|\|F_2\|\|$	$\cos(F_1,F_2)$
	Near the Fe edge (7112 eV)		
6875	4.81	1.28	1.0
6965	5.24	1.29	1.0
7030	5.83	1.30	1.0
7065	6.36	1.31	1.0
7084	6.89	1.32	1.0
7098	7.61	1.32	1.0
7104	8.18	1.32	1.0
	Near the Ni edge (8333 eV)		
8150	3.21	2.36	0.577
8250	3.04	3.08	0.544
8283	2.99	3.51	0.532
8302	2.96	3.98	0.525
8315	2.94	4.53	0.521
8322	2.93	5.01	0.519
8325	2.92	5.32	0.518

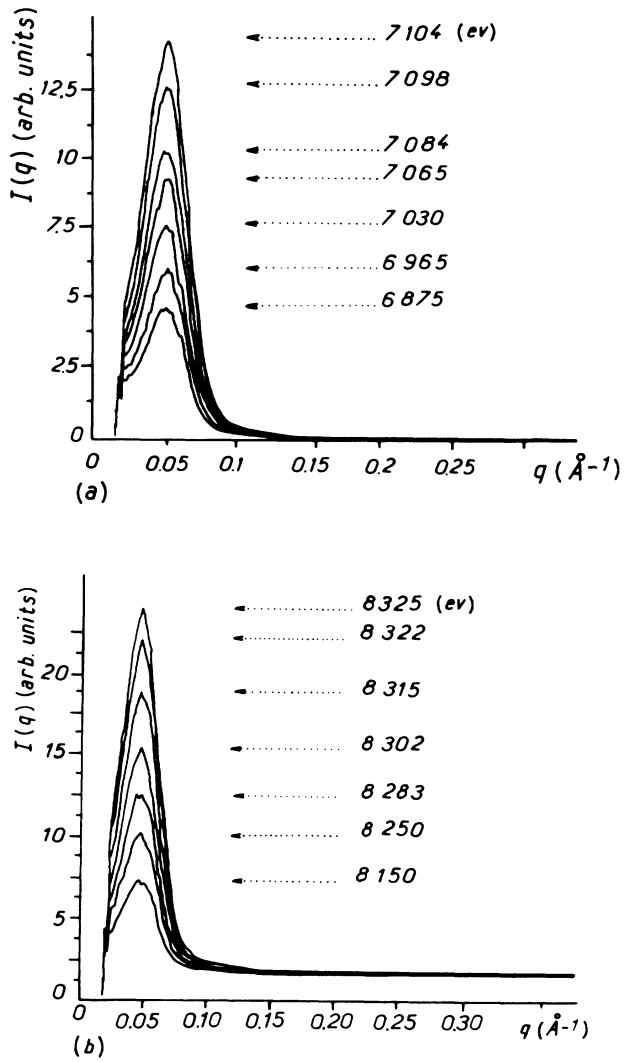

FIG. 1. Corrected experimental intensity vs q for the Cu-Ni-$Fe_{0.15}$ sample aged 56 h at 500 °C. (a) Near the Fe absorption edge. The different curves correspond to photon energies of 7104, 7096, 7084, 7065, 7030, 6965, and 6875 eV. (b) Near the Ni absorption edge. The different curves correspond to photon energies of 8325, 8322, 8315, 8302, 8283, 8250, and 8150 eV. The Fe fluorescence has not been removed to show its relative importance.

were multiplied by a factor depending only on the energy: this is illustrated by the absence of any clear shift in their peak position. This same shape and variation with energy of the curves is observed for other aging times (3 h, 9 h), except for the as-quenched state where the scattering is rather flat (Fig. 2). Therefore, the following analysis is significant in all cases where the signal was sufficient, namely for aging longer than 1 h. The kinetics will be discussed later on.

To check the consistency of the data, we have calculated $\sum_q I(q,E)$ for a given energy and plotted the resulting values as a function of $F_1 = |f_{Cu} - f_{Fe}|$ or $F_2 = |f_{Cu} - f_{Ni}|$. In Figs. 3(a) and 3(b) these variations are

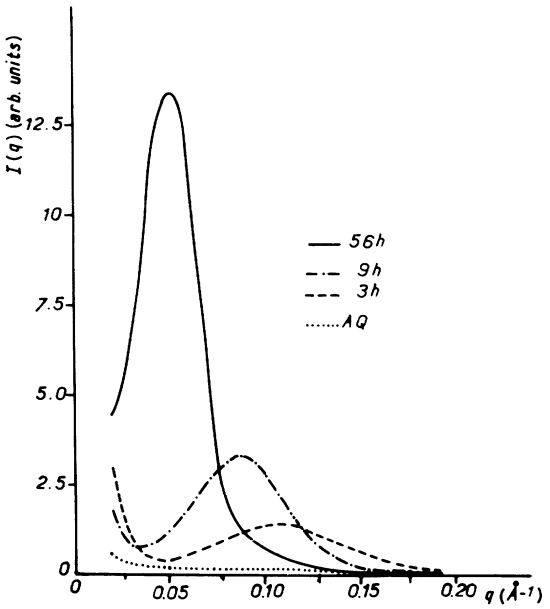

FIG. 2. Kinetics of the average scattering cross section in Cu-Ni-$Fe_{0.15}$ aged at 500 °C (photon energy 7104 eV).

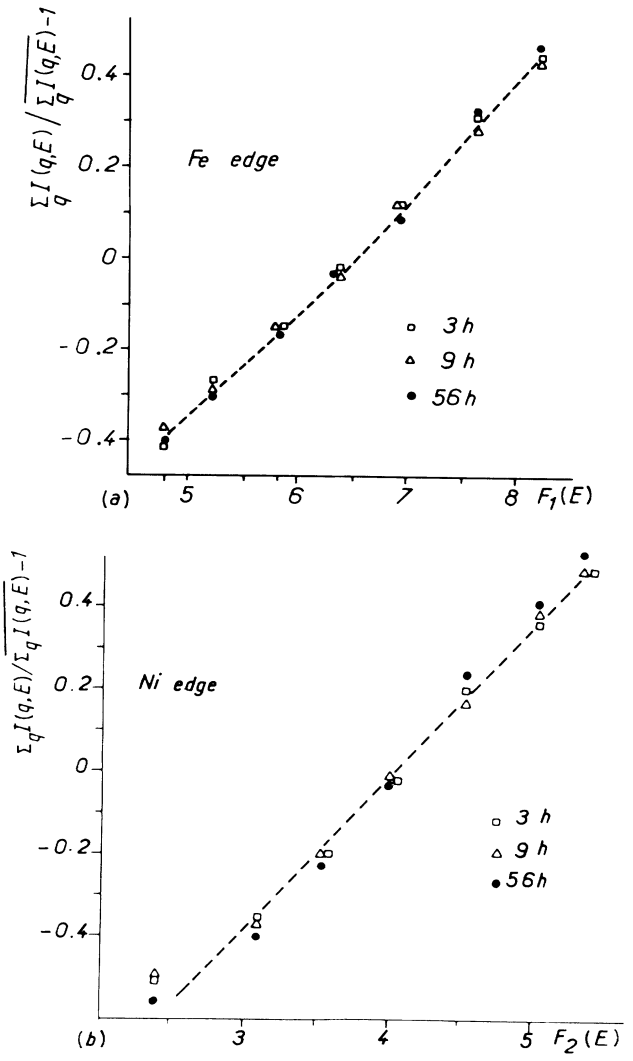

FIG. 3. Intensity curves (summed over a given q range) vs the variation of atomic scattering factor difference (for easy comparison, relative variations are plotted): (a) near the Fe edge (in abscissa $|f_{Cu}-f_{Fe}|$); (b) near the Ni edge (in abscissa $|f_{Cu}-f_{Ni}|$).

represented for the three different aging times of the same alloy unmixed at 500 °C.

At first glance, these variations versus F_1 or F_2 are rather smooth, almost linear. In particular, no point (except maybe the lowest energy at the Ni edge) shows any deviation from a regular behavior. From these plots, the precision of our data can be estimated roughly within 2%. A more precise observation of Fig. 3(a) (Fe edge) shows a slight curvature of the plot while it is indistinguishable near the Ni edge, Fig. 3(b). In any case, this curvature is so weak that three parameters [the $S_{ij}(q)$ or the sum $\sum_q S_{ij}(q)$] cannot be safely extracted from data obtained on a single edge.

As was already mentioned, we have extracted the $S_{ij}(q)$ functions through a minimization of $\mathcal{N}(q)$ [see Eq. (10)] and, in general, without imposing any conditions on the $S_{ij}(q)$ signs. Some corresponding results are gathered in Figs. 4(a)—(4(c), where drawn are the three homoatomic $S_{ii}(q)$ plus the $S_{\text{Fe-Ni}}$ one. Let us remark that these four PSF are not linearly independent since $\sum_j S_{ij}(q)=\delta(q)$.

The obtained PSF are not unphysical because all the S_{ii} are positive and because obviously the $S_{ij}^2-S_{ii}S_{jj}\leq 0$ relation is fulfilled. Before any discussion concerning Fig. 4, we had to check how confident in our results we could be. First we compared the experimental scattered intensities to the one recalculated [with Eq. (6)] from the $S_{ij}(q)$ that we had determined. From Figs. 5(a) and 5(b), as an example, we see that both match fairly well. But this was expected since, from the ill-conditioning of the matrix, we know that the minimum of $\mathcal{N}(q)$ was not very deep.

Then we varied the number of different energies put into the minimization: up to only two different energies on each edge, there is no qualitative change, the PSF becoming more wiggly but still comparable. Only when using data collected on a single edge [the Fe one in Figs. 6(a) and 6(b)] did it make a big difference: we had to impose the signs of S_{ii}'s to be positive, and even so the reconstructed intensities, although correct on the Fe edge, were completely false on the Ni one. After this, we checked the influence of the data precision by multiplying each $I(q,E)$ by a random factor with an average equal to 1 and a mean-square deviation set to 5%. Although the general shape of the resulting $S_{ij}(q)$ was comparable, the curves show much extra dispersion. Our last test was the multiplication of f' and f'' by a random factor, still with

a 5% square deviation. The resulting plots of $\sum_q I(q,E)$ variations versus F_1 do not show as smooth a behavior as it did before. But even so, the $S_{ij}(q)$ are not qualitatively changed, although the reconstructed curves deviate much more from the experimental data (Fig. 7).

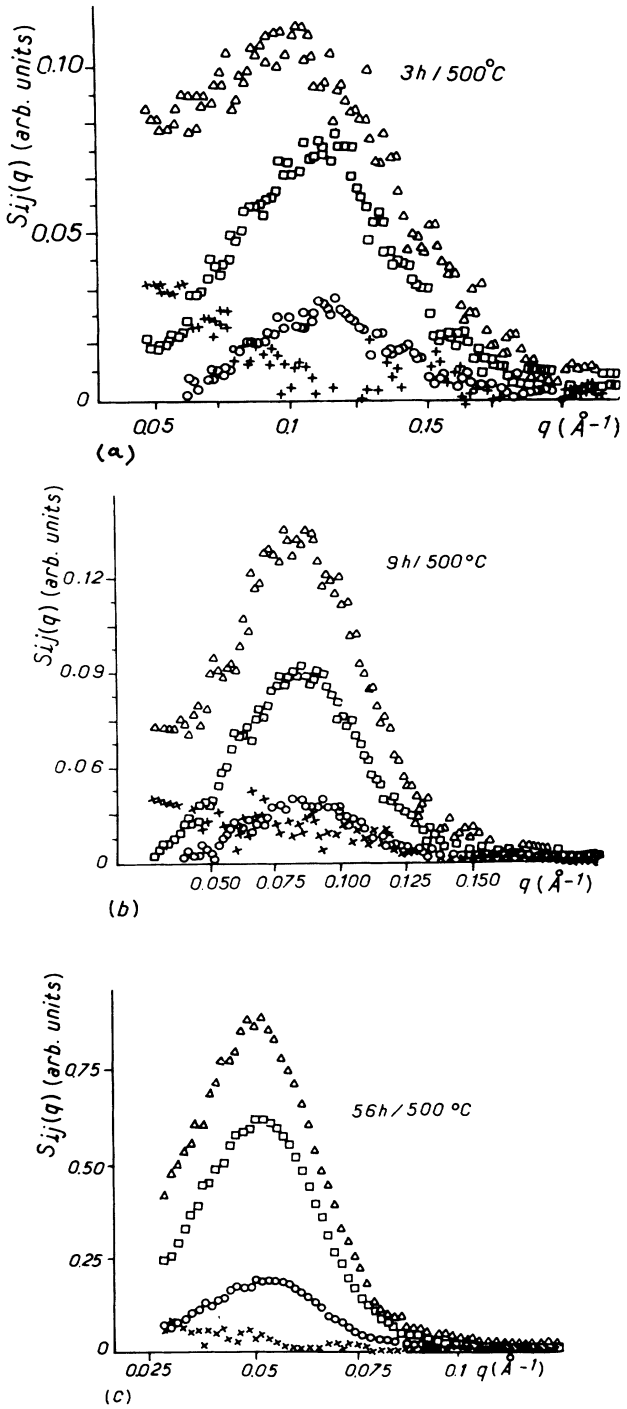

FIG. 4. Calculated partial structure factors for different aging times at 500 °C of Cu-Ni-$Fe_{0.15}$: $S_{Cu\text{-}Cu}$ (open triangle); $S_{Ni\text{-}Ni}$ (open square); $S_{Fe\text{-}Fe}$ (open circle); $S_{Ni\text{-}Fe}$ (plus). (a) After aging 3 h; (b) 9 h; (c) 56 h.

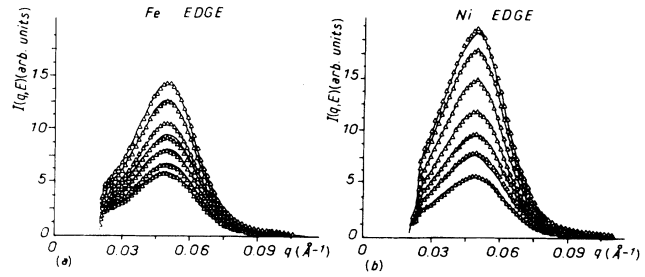

FIG. 5. Comparison of experimental intensities [lines (cf. Fig. 1)] and the intensities calculated from partial structure factors of Fig. 4(c) (triangles).

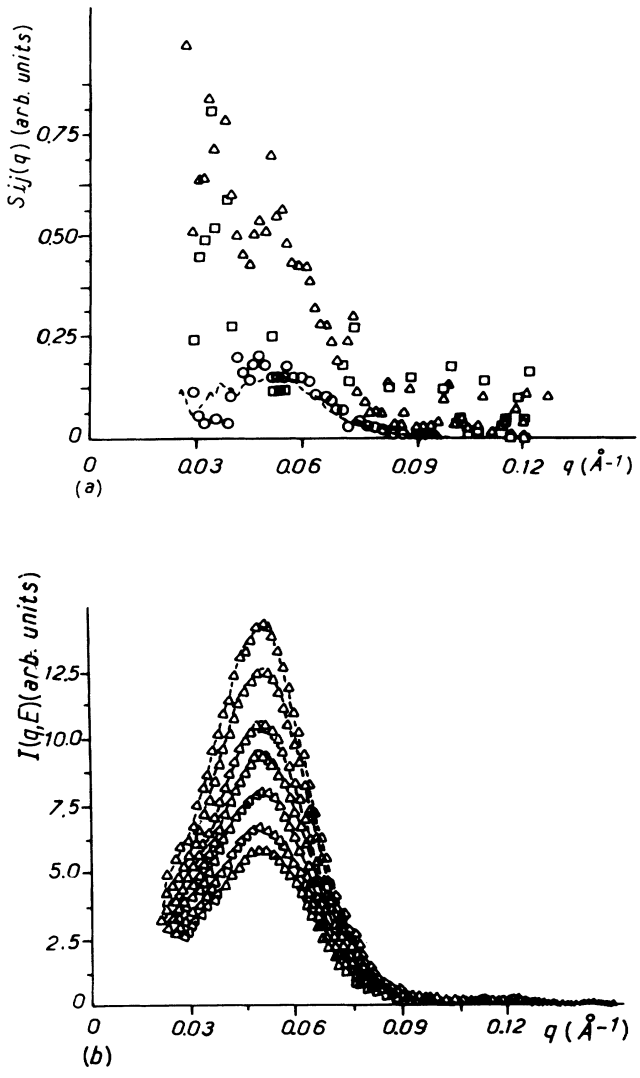

FIG. 6. Analysis of anomalous data near the Fe edge only (case of aging: 56 h at 500 °C): (a) calculated PSF, the $S_{Ni\text{-}Ni}$ PSF has been constrained to be positive (same symbols as in Fig. 4); (b) reconstructed intensities (triangles) and experimental data (lines).

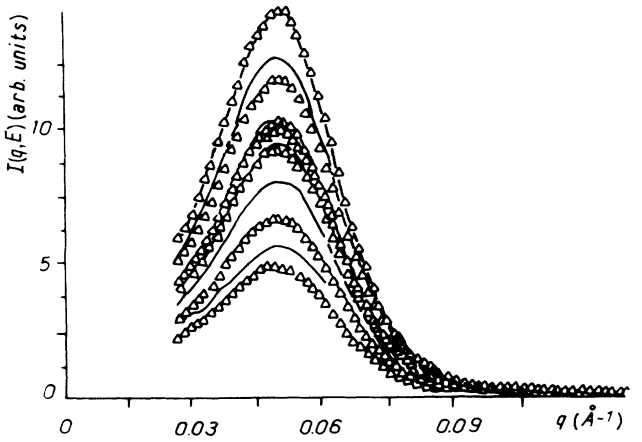

FIG. 7. Influence of a random error of 5% in the knowledge of f' (see text): same notations as in Fig. 5.

V. PARTIAL STRUCTURE FUNCTIONS: ANALYSIS AND DISCUSSION

For the three aging times, 3, 9, and 56 h, the PSF curves [Figs. 4(a)—4(c)] show similar behavior, the $S_{\text{Fe-Ni}}$ being close to zero on the entire q range. $S_{\text{Cu-Cu}}$, $S_{\text{Ni-Ni}}$, and $S_{\text{Fe-Fe}}$ curves present well-defined maxima and, at the first glance, they appear homothetic (and they are also quite homothetic with the intensity curves). Their related ratios do not vary with the aging time ($S_{\text{Fe-Fe}}/S_{\text{Cu-Cu}} \sim 0.2 \pm 0.03$; $S_{\text{Ni-Ni}}/S_{\text{Cu-Cu}} \sim 0.62 \pm 0.07$).

A. Comparison between PSF and unmixing model predictions

The simplest model is obviously the two-phase one, which is supported by previous studies, as detailed in the Introduction. From Eqs. (6) and (8) the ASAXS intensities can be written as

$$I(q,E) = [F_1^2(E)(\Delta C_1)^2 + 2F_1(E)F_2(E)\cos\varphi(E)\Delta C_1 \Delta C_2 + F_2^2(E)(\Delta C_2)^2] S_{pm}(q) \ . \quad (11)$$

Obviously, the $\sum_q I(q,E)$ variations versus $F_1(E)$ or $F_2(E)$ depend only on two parameters, $\Delta C_1 \sum_q S_{pm}(q)$ and $\Delta C_2/\Delta C_1$ which is the tie-line slope. We have determined the values of $\Delta C_2/\Delta C_1$, fitting Eq. (11) with data near a single edge. The tie-line slopes deduced from data near one edge or near the other one show a discrepancy far beyond data uncertainty (Table II).

TABLE II. Tie-line slope deduced from ASAXS data near a single edge.

Aging time	$\Delta C_2/\Delta C_1$ (Fe edge)	$\Delta C_2/\Delta C_1$ (Ni edge)
3 h	1.25	2.01
9 h	1.61	1.93
56 h	1.05	2.69

From results on the Fe edge, we have calculated the values of $\sum_q I(q,E)$ on the Ni edge which are in disagreement with experimental data by a factor between 1.5 and 2. Moreover, the relation $S_{12}(q)^2 - S_{11}(q)S_{22}(q) = 0$ is obviously not fulfilled, and this on the whole q range.

Another way to exemplify this disagreement with the two phase model is to look at the PSF locus in the $S_{00}(q)$, $S_{11}(q)$, and $S_{22}(q)$ referential frame. Two orthogonal projections $S_{00}(q)$, $S_{11}(q)$ and $S_{00}(q)$, $S_{22}(q)$ are drawn, respectively, in Figs. 8(a) and 8(b) (case of 56 h at 500 °C). They define a smooth curve in the $3d$ space; since they are not located on a straight line, they cannot be proportional to the same $S_{pm}(q)$ function and the further step is to check how many of these $S_{ii}(q)$ are linearly independent. For that purpose, the closest plane in the $3d$ PSF space was computed with the condition that $\sum_q [\sum_i \alpha_i S_{ii}(q)]^2$ was minimum (α_i being the direction cosines). Shown in Fig. 9 is the S_{ii} locus near the closest plane: bars indicate the distance between the locus and the plane (magnified by a factor of 10). The S_{ii} locus being nearly in the projection plane, two independent $S_{ii}(q)$ are obviously sufficient to describe the scattering. The orientation of this

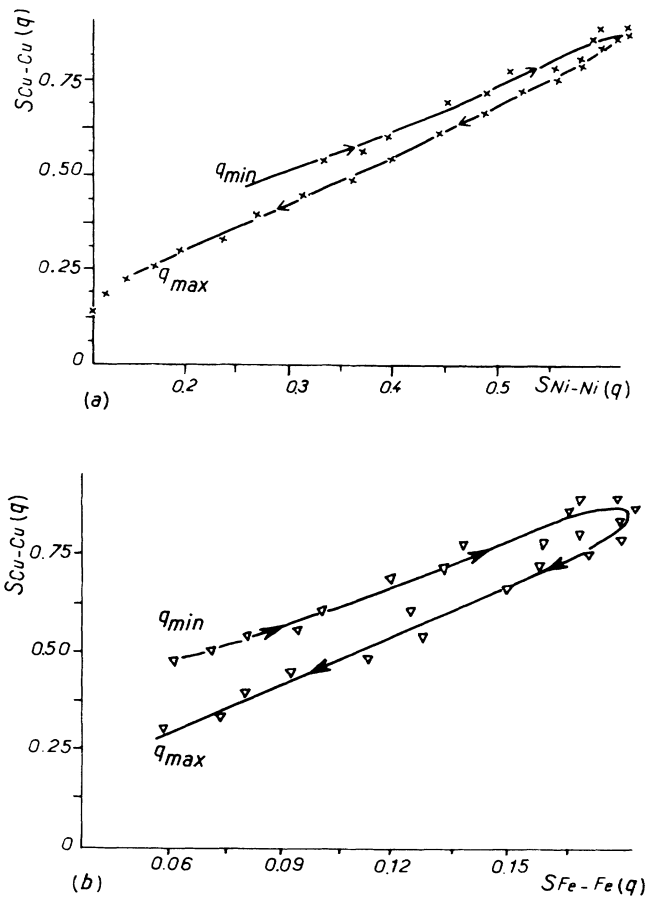

FIG. 8. Locus of PSF data drawn in the "PSF space" (case of 56 h at 500 °C: (a) $S_{\text{Cu-Cu}}$ vs $S_{\text{Ni-Ni}}$; (b) $S_{\text{Cu-Cu}}$ vs $S_{\text{Fe-Fe}}$.

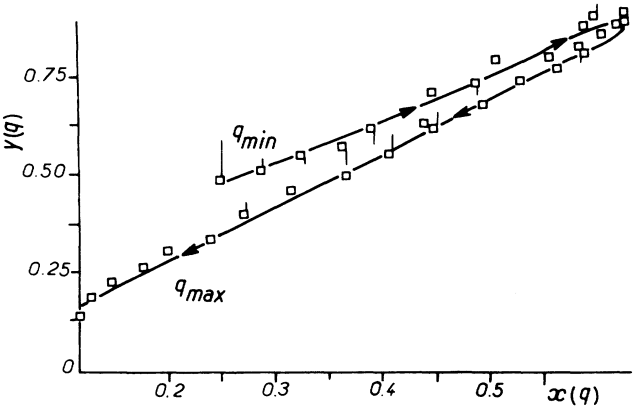

FIG. 9. Data of Fig. 8 replotted in the projection plane. The bar attached to each experimental point (squares) is the distance to the plane (the scale has been magnified by a factor of 10).

plane does not depend of the aging time after 3 h of aging ($\theta=81°\pm2°$; $\varphi=31°\pm2°$ with respect to the $S_{\text{Cu-Cu}}$ axis). This orientation is completely different from the one defined by $S_{\text{Ni-Fe}}=0$ (i.e., $S_{00}-S_{11}-S_{22}=0$). The intersection of these two planes gives a straight line corresponding to the $S_{\text{Fe-Fe}}/S_{\text{Cu-Cu}}$ and $S_{\text{Ni-Ni}}/S_{\text{Cu-Cu}}$ ratios noticed in the previous paragraph. There is not a single independent S_{ii} for this one should be the two-phase one. Nevertheless, there is a dominating one which gives the principal S_{ii} direction and a secondary one which fixes the projection plane.

Since the two-phase model does not work, we tried the case of two different kinds of precipitates. But, as explained below, such hypothesis is not consistent with our results. Indeed, if we look at Eqs. (8) and (9), there are only two possibilities: firstly, the two kinds of precipitates are uncorrelated [then $\psi_{12}(q)=0$ in Eq. (8)]. From $S_{12}(q)\simeq0$ and from Eq. (9), we can deduce from this that the two corresponding tie lines should have opposite signs: one kind of precipitates should be enriched in the two solute elements when the other should be enriched in one sort and depleted in the other. But this is not compatible with the miscibility gap as extrapolated from high-temperature data through a thermodynamic calculation of the metastable fcc ternary phase diagram:[8] the three-phase system which may have developed consists of a Cu-rich phase and two NiFe ones. The two last phases are a Ni_3Fe ordered phase and a disordered one of composition slightly different. This characteristic gives tie lines which have similar slopes, of the order of 3. The second possibility is that the two kinds of precipitates are correlated. ψ_{12}, which represents the correlation between phases 1 and 2, cannot be a linear combination of the autocorrelation functions ψ_{11} and ψ_{22}: the three ψ_{ij} are then independent. However, because S_{ij} and ψ_{ij} are bound by linear equations [matrix λ of Eq. (9)], the λ matrix should then be singular. This implies once again that the two tie lines should be identical.

As an intermediate conclusion, this study of partial structure factors shows an unmixing morphology in Cu-Ni-Fe, more complicated than the two-phase system proposed by previous studies.

B. Kinetics of partial structure factors

During the unmixing of binary systems, the time evolution is generally described by a change of a characteristic "length" which may have several definitions. In nondilute systems with a well-defined maximum, the position of the maximum, q_m, is one way of defining, while the moments, q_n, are other ones. Let us recall the moment definition

$$q_n=\sum_0^{q_c} q^n S(q,t) \Big/ \sum_0^{q_c} S(q,t) ,$$

where q_c is an experimental cutoff which was chosen equal to $2q_m$ for homogeneity between all our results.

A first check of reliability of these kinetic experiments is the observation of the SAXS intensity after quench (Fig. 2), which is fairly flat, up to 0.35 Å^{-1}, without any visible hump. It indicates that the solid solution has been correctly retained during the water quench from 850 °C. At a given x-ray energy (for instance 7104 eV to have the best contrast), the I curves present the usual kinetic behavior. Their maximum increases and shifts towards low q values. The value of parameters q_m, q_1, q_2, and R_g as given by the standard SAS analysis is given in Table III. We have applied this same analysis to the PSF $S_{ii}(q)$ and we have found the corresponding values of q_m, q_1, and q_2 (Table IV). From this table comes the very surprising result, that, whatever the measurement of the characteristic length λ of the system (i.e., through q_m, q_1, or q_2), we systematically find $\lambda_{\text{Cu-Cu}}/\lambda_{\text{Ni-Ni}}>\lambda_{\text{Cu-Cu}}/\lambda_{\text{Fe-Fe}}>1$ with a ratio equal to 1.09 ± 0.05, 1.04 ± 0.02, and 1.02 ± 0.02 after 3, 9, and 56 h at 500 °C, respectively. This significant shift in peak position indicates that the characteristic lengths for the different autocorrelation functions CuCu, NiNi, FeFe are slightly different.

Unmixing kinetics are generally expressed in terms of power laws

TABLE III. Analysis of kinetics of SAS intensity during isothermal aging of Cu-Ni-$Fe_{0.15}$ at 500 °C.

Aging time	I_m (7104 eV)	q_m (nm^{-1})	q_1 (nm^{-1})	q_2/q_1^2	R_g (nm)
1 h	6.4	1.33	1.46	1.15	1.4
3 h	14	1.09	1.09	1.13	2.4
9 h	34	0.87	0.885	1.15	3.35
56 h	142	0.51	0.53	1.15	5.6

TABLE IV. Isothermal evolution of the characteristic PSF lengths.

Aging time	$S_{Cu\text{-}Cu}$ q_m (nm^{-1})	q_1 (nm^{-1})	q_2 (nm^{-2})	$S_{Ni\text{-}Ni}$ q_m	q_1	q_2	$S_{Fe\text{-}Fe}$ q_m	q_1	q_2
3 h	1.03	1.08	1.27	1.15	1.13	1.37	1.18	1.17	1.44
9 h	0.827	0.856	0.792	0.864	0.879	0.829	0.882	0.895	0.852
56 h	0.504	0.521	0.292	0.514	0.526	0.296	0.533	0.534	0.304

$q_1 = t^{-a}$, $q_m = t^{-a'}$, $I_m = t^{a''}$.

Although we realize that a kinetic study with only three different aging times may seem a bit short, we nevertheless tried it and obtained the following power-law exponents (Table V) with a correlation always better than 0.998. The most striking feature is that the three coefficients a' or the three a'' corresponding to the three types of PSF are identical within the limit of error. Of course, the values deduced from the intensity data at a given energy (7104 eV) also give the same results. The kinetics of the three PSF being the same, this explains why SANS intensities show an ordinary pseudobinary behavior, without presenting any bimodal regime, for instance. Moreover, our a' and a'' coefficients are well inside the range found in binary systems ($0.17 < a' < 0.33$ and $0.5 < a'' < 1$). They are in agreement with previous SANS studies[5] of unmixing of Cu-Ni-$Fe_{0.08}$ and Cu-Ni-$Fe_{0.04}$ ($0.2 < a' < 0.3$ and $0.7 < a'' < 0.9$). They can also be compared to the Monte Carlo simulation of the unmixing of binary alloys[21] from which was deduced $a = 0.23$ for a 50% alloy aged at $0.8T_c$ and $a = 0.25$ at $0.9T_c$. However, they found a q_2/q_1^2 ratio somewhat different: 1.19 at $0.8T_c$ and 1.27 at $0.9T_c$ when our results yielded 1.08. But since our cutoff was chosen at $2q_m$ for practical reasons, we may expect its influence to be greater on q_2 than on q_1^2, leading to an underestimation of their ratio. Another possible reason of such a discrepancy is due to the averaging on all orientations of a very anisotropic scattering (corresponding to the unmixing strongly oriented along ⟨100⟩ directions). A modification of this ratio has already been observed in a previous study on Al-Zn when a change occurs from spherical Guinier-Preston zones to (111) platelets.[22]

The last row of Table V needs comment: $a'' - 3a'$ is exactly null in a coarsening process whatever its nature, coagulation or evaporation condensation of the Lifschitz-Sluyzov type. Indeed, in concentrated binary systems, this relation was generally followed experimentally or was deduced from the theoretical analysis of late stages of unmixing. Another check that the unmixing stage in our case corresponds to a late stage, is to measure the integrated intensity which would then be nearly constant. In fact, the integrated intensity should be measured on the entire

TABLE V. Power-law coefficients of the PSF kinetics.

	$S_{Cu\text{-}Cu}$	$S_{Ni\text{-}Ni}$	$S_{Fe\text{-}Fe}$
$a \simeq a'$	0.25	0.26	0.27
a''	0.80	0.82	0.78
$a'' - 3a'$	0.05	0.04	−0.03

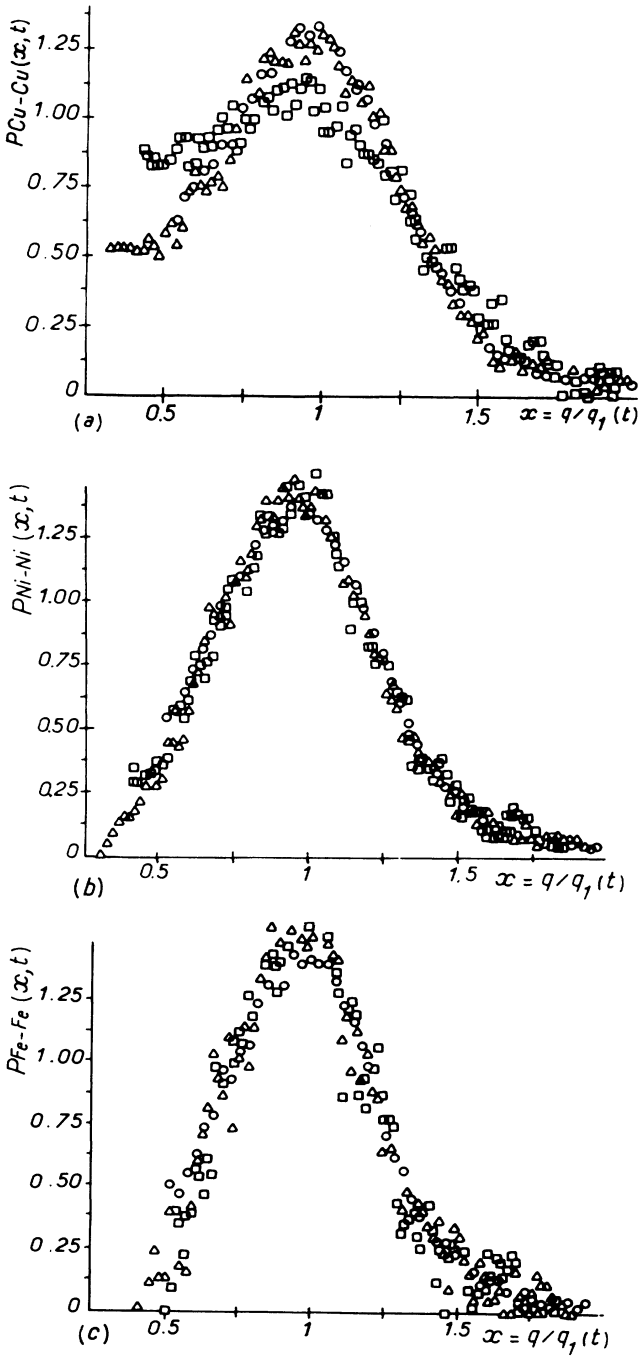

FIG. 10. Scaled partial structure factors (see text) for the three aging times 3 h (squares), 9 h (triangles), and 56 h (circles): (a) $P_{Cu\text{-}Cu}$; (b) $P_{Ni\text{-}Ni}$; (c) $P_{Fe\text{-}Fe}$.

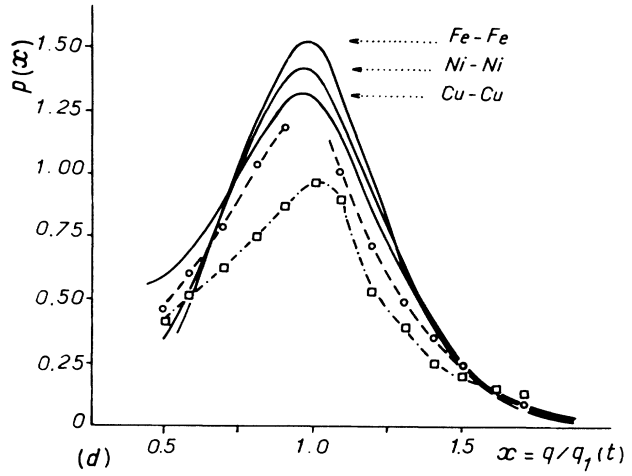

FIG. 11. Comparison with Lebowitz scaling (Ref. 21). Circles and dotted line $c=0.5$, $T/T_c=0.8$; squares and dashed-dotted line $c=0.5$, $T/T_c=0.9$.

first Brillouin zone and the precipitate contribution should be separated from the Laue's one following Gerold's analysis.[23] Unfortunately, this cannot be determined precisely enough, the q range (up to $2q_m$) being insufficient. Nevertheless, the troncated integrated intensity is rather constant (within $\pm 20\%$), giving indications that our aging times should be considered as a "late" stage.

Another related test of late stages is the now classical scaling procedure. The scaled structure function is defined, following Ref. 2, by

$$P(x,t)=q_1^3(t)S(q,t)/\sum_0^{q_c} S(q,t)q^2dq \ ,$$

where $x=q/q_1(t)$.

The scaled PSF $P_{\text{Cu-Cu}}$, $P_{\text{Ni-Ni}}$, and $P_{\text{Fe-Fe}}$ are shown in Figs. 10(a)—10(c). As can be seen, the scaled PSF are indeed independent of the aging time and, moreover, the three scaled PSF P_{ii} are pretty much the same. This result is not surprising since slight differences in the q_m position between the $S_{ii}(q)$ are lost during this data processing. Finally, the scaled function from the intensity spectra (which are themselves linear combinations of quasihomothetic PSF) has the same shape as the previously scaled PSF curves. As a comparison we have drawn together with the scaled PSF, the scaled functions deduced from Monte Carlo simulations of the $3d$ Ising model[21] (one corresponding to a deep quench inside the binary miscibility gap and the other to a shallow quench) (Fig. 11). There is an overall agreement: our scaled PSF appear to be closer to the simulation of a deep quench; but this detailed comparison may not be significant since it is known that cutoff problems (value of q_c/q_m) as well as anisotropy effects[22] may slightly deform the scaled functions. In fact, scaling is not a sensitive test of the phase separation nature, being a renormalization of a curve (the intensity, or the PSF) which is already averaging the "precipitate size," spatial distribution, morphology, etc.

VI. CONCLUSION

From anomalous small angle scattering, we have determined the partial structure factors PSF in a Cu-Ni-$Fe_{0.15}$ alloy for different aging times ranging from 3 to 56 h at 500 °C. $S_{\text{Cu-Cu}}$, $S_{\text{Ni-Ni}}$, and $S_{\text{Fe-Fe}}$ curves have a shape similar to what is observed in binary systems, a hump which indicates a rather regular fluctuation of concentration. This hump increases and its maximum shifts towards low q values. The kinetics follow power laws $q_m=t^{-0.26}$; $I_m=t^{0.80}$. The scaling is obeyed for the three-scaled PSF which moreover can be superimposed in between. These features are observed in the late stages of unmixing of binary systems and indeed, in previous studies of Cu-Ni-Fe using classical small angle scattering, a consistent analysis of the unmixing process was done in terms of a pseudobinary system.

Nevertheless, we have seen throughout this work that the two-phase model could not account for our results, the main points being the following.

(i) The tie-line slope, as determined from data near one edge, was different from the one determined near the other edge, with a discrepancy incompatible with data uncertainties.

(ii) Following the two-phase model, there should be only one independent function which should be the structure function of the precipitates $S_{pm}(q)$, all $S_{ij}(q)$ being proportional with related ratios. Experimental results give, in fact, two independent PSF.

(iii) The expression $S_{ij}-S_{ii}S_{jj}$ should be null if the two-phase model holds: this obviously is not the case on the entire q range.

A possible explanation is that there is a phase separation between Cu and Ni-Fe in agreement with atom probe determinations and phase diagram computations. However, in the domains enriched in Ni and Fe, there is long-range partitioning, "killing" the $S_{\text{Fe-Ni}}$ PSF amplitude, which, without changing much the S_{ii} shapes, modify their relative amplitude. This first determination of partial structure factors by anomalous small-angle scattering emphasizes that considering the unmixing of ternary systems in term of quasibinary ones, may only be a first-order approximation.

ACKNOWLEDGMENTS

The authors express their thanks to Mr. Gros for his essential help and to Mr. and Mrs. Allibert for their advice on sample preparation. They also thank their colleagues, Mrs. F. Bley and F. Livet, for their participation during the experiment and further discussions.

[1] J. D. Gunton, M. San Miguel, and P. S. Sahni, in *Phase Transitions and Critical Phenomena,* edited by C. Domb and J. M. Lebowitz (Academic, London, 1983), Vol. 8.

[2] K. Binder and D. W. Heermann, *Scaling Phenomena in Disordered Systems* (Plenum, New York, 1985).

[3] R. J. Livak and G. Thomas, Acta Metall. **19**, 497 (1971).

[4] V. Perovic, G. R. Purdy, and L. M. Brown, Scr. Metall. **15**, 217 (1981).

[5]M. Hillert, M. Cohen, and B. L. Averbach, Acta Metall. **9**, 536 (1961).
[6]W. Wagner, R. Poerschke, and H. Wollenberger, in *Decomposition of Alloys: The Early Stages,* Proceedings of the Second Acta Scripta Metallurgica Conference, Sonnenberg, 1983 (Pergamon, New York, 1984), p. 170.
[7]J. Piller, W. Wagner, H. Wollenberger, P. Mertens, *Decomposition of Alloys: The Early Stages,* Ref. 6, p. 156.
[8]T. G. Chart, D. G. Gohil, X. Zhong Shu (unpublished).
[9]P. H. Fuoss, P. Eisenberger, W. K. Warburton, and A. Bienestock Phys. Rev. Lett. **46**, 1537 (1981).
[10]P. Goudeau, A. Fontaine, A. Naudon, and C. E. Williams, J. Appl. Crystallogr. **19**, 19 (1986).
[11](a) J. J. Hoyt, O. Lyon, J. P. Simon, B. Clark, B. E. C. Davis, and D. de Fontaine, Solid State Commun. **57**, 3 (1986); (b) O. Lyon, J. J. Hoyt, R. Pro, B. E. C. Davis, B. Clark, D. de Fontaine, and J. P. Simon, J. Appl. Crystallog. **18**, 480 (1985).
[12]O. Lyon and J. P. Simon, Acta Metall. **34**, 1197 (1986).
[13]J. P. Simon and O. Lyon, Philos. Mag. Lett. (to be published).
[14]J. P. Simon, O. Lyon, and D. de Fontaine, J. Appl. Crystallogr. **18**, 230 (1985).
[15]D. de Fontaine, in *Solid State Physics,* edited by H. Ehrenreich, F. Seitz, and D. Turnbull (Academic, New York, 1979), Vol. 34, p. 73.
[16]N. J. Schevchick, Philos. Mag. **35**, 805 (1977).
[17]M. Bessenay, Ph.D thesis, University of Paris 6, 1985.
[18]T. G. Munro, Phys. Rev. B **25**, 5037 (1982).
[19]J. M. Dubuisson, J. M. Dauvergne, C. Depautex, P. Vachette, and C. E. Williams, Nucl. Instr. Meth. A **246**, 636 (1986).
[20]S. Sasaki (unpublished).
[21]J. L. Lebowitz, J. Marro, and M. H. Kalos, Acta Metall. **30**, 297 (1982).
[22]J. P. Simon, P. Guyot, and A. G. de Salva, Philos. Mag. A **49**, 151 (1984).
[23]V. Gerold, J. Appl. Crystallogr. **10**, 25 (1979).